Theor Chem Acc (2011) 130:269–277
DOI 10.1007/s00214-011-0974-0

REGULAR ARTICLE

Structures and bonding situation of Pb_2X_2 (X = H, F, Cl, Br and I)

Taka Shimizu · Gernot Frenking

Received: 10 May 2011 / Accepted: 2 June 2011 / Published online: 28 June 2011

Abstract Quantum chemical calculations using DFT (BP86) and ab initio methods (MP2, MP4 and CCSD(T)) have been carried out for the title compounds. The nature of the Pb–Pb interactions has been investigated with an energy decomposition analysis. The energy minimum structures of the halogen substituted Pb_2X_2 molecules possess a doubly bridged butterfly geometry **A** like the parent system Pb_2H_2. The unusual geometry can be explained with the interactions between PbX fragments in the $X^2\Pi$ ground state which leads to one Pb–Pb electron-sharing σ bond and two donor–acceptor bonds between the Pb–X bonds as donor and vacant $p(\pi)$ AOs of Pb. The energy difference between the equilibrium form **A** and the linear structure XPb≡PbX (**E**) which is a second-order saddle point is much higher when X is a halogen atom than for X = H. This is because the $a^4\Sigma^- \leftarrow X^2\Pi$ excitation energies of PbX (X = F–I) are higher than for PbH. The structural isomers **B**, **D1**, **D2**, **E**, **F1**, **F2** and **G** of Pb_2X_2 are no minima on the potential energy surface.

Keywords Diplumbaacetylene · Bonding analysis · Ab initio calculations · DFT calculations

1 Introduction

The heavy-atom analogues of acetylene E_2H_2 and their substituted derivatives E_2R_2 (E = Si–Pb) have fascinated researchers for a long time due to their unusual structures [1–3]. The first results came from theoretical studies of Si_2H_2. In 1982, Moskowitz et al. [4] revealed that the linear structure of Si_2H_2 is not an energy minimum structure, which shows a fundamental difference of Si_2H_2 from acetylene. In 1983, Lischka and Köhler [5] and Binkley et al. [6] reported that the singlet potential energy surface (PES) of Si_2H_2 is quite different from that of C_2H_2. These reports predicted that a non-planar doubly bridged structure is the global energy minimum on the Si_2H_2·PES, whereas the acetylene-like linear species HSi≡SiH is a second-order saddle point. Subsequent theoretical studies of Si_2H_2 and Ge_2H_2 isomers at higher levels of theory [7–25] confirmed that the non-planar doubly bridged structure is the global minimum for E_2H_2 (E = Si, Ge). In more recent times, theoretical studies of Pb_2H_2 [21, 26–28] showed that the non-planer doubly bridged butterfly structure is also the lowest-lying isomer of the lead homologue. The theoretical results agree with the results of spectroscopic investigations of E_2H_2 in low-temperature matrixes [29–32].

The theoretical investigations dominated the study of E_2R_2 molecules for a long time, until Power et al. made a breakthrough in the experimental research in 2000 [33]. They synthesized the substituted lead compound R*PbPbR* with bulky terphenyl substituents R* (R* = C_6H_3-2,6-$Trip_2$; Trip = C_6H_2-2,4,6-$^i Pr_3$; Pr = propyl) and they identified its geometry by X-ray structure analysis. The synthesized isomer does not have a butterfly structure, but a trans-bent geometry. A peculiar aspect of the molecular structure is the rather long Pb–Pb distance of 3.188 Å and the acute C–Pb–Pb bond angle of 94.3°. The authors suggested that the compound R*PbPbR* has a Pb–Pb single bond where the Pb–Pb bond length is longer than the typical single bond and where each PbR* fragment carries a σ electron lone-pair. A following theoretical study by Frenking et al.

Dedicated to Professor Shigeru Nagase on the occasion of his 65th birthday and published as part of the Nagase Festschrift Issue.

T. Shimizu · G. Frenking (✉)
Fachbereich Chemie, Philipps-Universität Marburg,
Hans-Meerwein Strasse, 35032 Marburg, Germany
e-mail: frenking@chemie.uni-marburg.de

[27] showed that the structure of the synthesized isomer R*PbPbR* conforms to a higher-lying form of Pb_2H_2 which is a transition state for the parent compound which becomes an energy minimum through the repulsive interactions of the bulky substituents. After the theoretical study by Frenking et al. [27], Power et al. [34] reported an MO analysis of MePbPbMe. The report revealed that the orbitals of the trans isomer for Pb_2H_2 are similar to those of Pb_2Me_2.

Theoretical investigations were carried out to understand the nature of the E–E bonding. Lein et al. [35] addressed the question why the heavy-atom homologues of acetylene HEEH where E = Si–Pb are not linear but rather possess unusual equilibrium structures. They could show that the answer to the question can be given when the electronic state of the interacting EH moieties are considered. The further investigated the E–E interactions in E_2H_2 by an Energy Decomposition Analysis (EDA). Not many studies have been reported about E_2R_2 where R is an electron-donating group R [36, 37]. Also, there are only few studies devoted to E_2X_2 isomers containing electron-withdrawing groups X [38, 39]. To the best of our knowledge, there have been no experimental studies of Pb_2X_2 molecules.

In this work, the results of theoretical investigations of Pb_2X_2 molecules with electron-withdrawing groups X = H, F, Cl, Br, I are presented. Scheme 1 shows the singlet isomers of Pb_2X_2 investigated here. The calculated isomers are denoted as non-planar doubly bridged structure (**A**), singly bridged planar structure (**B**), vinylidene structure (**C**), trans-bent structure with different electronic states (**D1** and **D2**), linear structure (**E**), cis-bent structures (**F1** and **F2**) and as planar doubly bridged structure (**G**).

2 Methods

The geometries of the molecules have been optimized at the DFT level of theory using the exchange functional of Becke [40] with the correlation functional of Perdew (BP86) [41, 42]. Uncontracted Slater-type orbitals (STOs) were used as basis functions for the SCF calculations [43]. The basis sets have quadruple-ζ quality augmented by four sets of polarization functions, i.e. two *p* and two *d* functions on hydrogen and two *d* and two *f* functions on the other atoms. This level of theory is denoted BP86/QZ4P. An auxiliary set of *s*, *p*, *d*, *f*, *g* and *h* STOs was used to fit the molecular densities and to represent the Coulomb and exchange potentials accurately in each SCF cycle. Scalar relativistic effects have been considered using the zero-order regular approximation (ZORA) [44]. The nature of the stationary points on the potential energy surface was characterized by calculating the Hessian matrices. The calculations were carried out with the program package ADF [45].

The relative energies of singlet isomers have also been calculated at MP2 [46], SCS-MP2 [47], MP4 [48] and CCSD(T) [49–51], with Dunning's correlation-consistent quadruple zeta basis sets augmented by diffuse functions (aug-cc-pVQZ) [52–54] in conjunction with a quasi-relativistic effective core potential for Pb [55]. The calculations of adiabatic excitation energies were carried out with MRCI-SD/CASSCF [56–58] and MRCI-SD(Q)/CASSCF with aug-cc-pVQZ basis set [52, 54], where (Q) means the Davidson correction [59]. The program package MOLPRO 2006 [60] was used for the MP2, SCS-MP2, MP4, CCSD(T) and MRCI-SD calculations.

EDA calculations were carried out at the BP86/QZ4P level of theory using ADF 2007. In the EDA, the isomers of **A**, **B**, **D1**, **D2**, **E**, **F1**, **F2** and **G** of Pb_2X_2 molecules are divided into two EX fragments to analyse the E–E bonding situation which is the same procedure as in our previous report [35]. The EDA makes it possible to divide the bonding energy of a chemical bond into some energy contributions and to obtain a quantitative interpretation of chemical bonds. The EDA is based on the energy partitioning scheme of Morokuma [61] and Ziegler and Rauk [62].

The bond formation energy ΔE of AB from two fragments A and B is divided in two steps. In the first step, the fragments A and B are deformed from their equilibrium geometry to their geometries and electronic state in the final complex AB. The energy requiring in this step is the preparation energy (ΔE_{prep}).

$$\Delta E = -D_e = \Delta E_{\text{prep}} + \Delta E_{\text{int}}. \quad (1)$$

In the second step, the electronic interaction energy (ΔE_{int}) between fragment A and fragment B is estimated. The interaction energy ΔE_{int} is divided into three terms.

$$\Delta E_{\text{int}} = \Delta E_{\text{elstat}} + \Delta E_{\text{pauli}} + \Delta E_{\text{orb}}. \quad (2)$$

The first term, ΔE_{elstat}, is the electrostatic energy, which comes from the interaction between fragments A and B

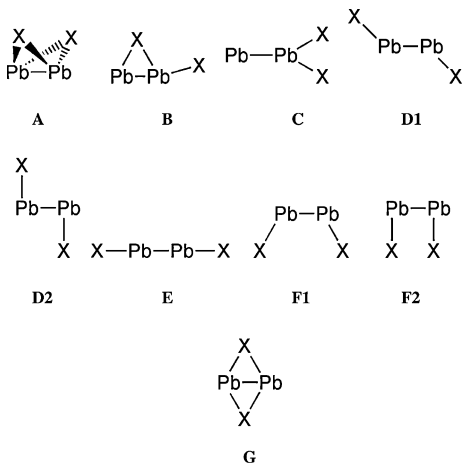

Scheme 1 Overview of the investigated isomers of Pb_2X_2

with fixed electronic states in the geometry of AB. The second term in Eq. 2, ΔE_{pauli}, is the Pauli repulsion, which is the energy to antisymmetrize and reorthogonalize the wave function of complex $\Psi_{AB} = \hat{A}N\Psi_A\Psi_B$ from Kohn–Sham orbitals of Ψ_A and Ψ_B. The last term in Eq. 2, ΔE_{orb}, is the orbital interaction energy, which is produced in the relaxation from the determinant $\Psi_{AB} = \hat{A}N\Psi_A\Psi_B$ to the final Kohn–Sham determinant Ψ_{AB}^{min}. The orbital interaction energy contains both inter- and intrafragmental relaxation effects.

The figures of all Pb_2X_2 isomers are drawn with ChemCraft [63].

3 Geometries and energies

Figure 1 shows the optimized geometries of the calculated isomers **A**–**G** of Pb_2X_2 (X = H, F, Cl, Br and I) at BP86/QZ4P. Table 1 gives the relative energies of the stationary points on the singlet potential energy surface calculated at different levels of theory using the BP86/QZ4P optimized geometries. The results for the hydrogen parents system are in agreement with previous calculations using DFT [21, 27, 28, 35] and ab initio methods [26].

The doubly bridged isomer **A** is predicted as global energy minimum form of Pb_2X_2 for all atoms X. This result is independent from the level of theory (Table 1). It is gratifying that the relative energies at all levels of theory which are employed in this work are quite similar. Calculations of the vibrational frequencies indicate that structure **A** is actually the only energy minimum structure of Pb_2X_2 for all atoms X. This has been shown before in a theoretical study of Pb_2H_2 [27]. The calculations which are presented here predict that the halogen substituted systems **B**–**G** are either transition states ($i = 1$) or higher-order saddle points on the PES. The energetically next low-lying structure of the halogen substituted compounds is **D2** which is for all halogen atoms X ~ 20 kcal/mol higher in energy than **A** (Table 1).

The calculated geometries for structure **A** show that the Pb–Pb distance becomes longer in the order H < F < Cl < Br < I. The trend, which could be caused by the increasing size of the halogen atoms, is opposite to most other isomers such as in **D2** where the Pb–Pb bond length for the halogen systems decrease with F > Cl > Br > I.

4 Analysis of the bonding situation

The theoretical study by Lein et al. [35] has shown that the unusual equilibrium structures **A**–**D,** and the finding that **E** is not an energy minimum form for HEEH (E = Si–Pb) can be explained with the relative energies of the $X^2\Pi$ electronic ground state and $a^4\Sigma^-$ first excited state of the EH fragment. We use the same approach for the discussion of the Pb_2X_2 structures which are further extended to the structures **F**, **G** (Scheme 1). Figure 2 shows schematically the two electronic states for PbX which are also the ground and electronic states for the halogen substituted systems. Table 2 gives the calculated $a^4\Sigma^- \leftarrow X^2\Pi$ excitation energies at BP86/QZ4P and at MRCI-SD/aug-cc-pvQZ as well as MRCI-SD(Q)/aug-cc-pvQZ using the BP86/QZ4P optimized bond lengths. There is very little known experimentally about the low-lying electronic states of PbX. All species with X = H, F, Cl, Br, I have a $X^2\Pi$ electronic ground state [64]. There are very early spectroscopic studies of PbH by Watson [65, 66] who observed complex bands in the red and infra-red region which were later suggested [67] to belong to the $a^4\Sigma^-$ states which are split by spin–orbit coupling. A more recent theoretical study gave calculated values of 49.2 and 58.1 kcal/mol for the $a^4\Sigma^-_{1/2} \leftarrow X^2\Pi$ and $a^4\Sigma_{3/2} \leftarrow X^2\Pi$ excitation which were compared with experimental values of 50.3 and 51.5 kcal/mol [68]. The latter data are in excellent agreement with our values of 50.7 kcal/mol (MRCI-SD(Q)/aug-cc-pVQZ) and 52.0 kcal/mol (BP86/QZ4P) which were calculated with neglecting spin–orbit coupling.

The data in Table 2 suggest that the $a^4\Sigma^- \leftarrow X^2\Pi$ excitation energies of the halogen systems PbX are even higher than for the parent compound PbH. Since the linear structure XPb ≡ PbX requires the highly excited $a^4\Sigma^-$ state of PbX to form a triple bond, the formation of isomer **E** of the halogen systems Pb_2X_2 is energetically even less favourable than for Pb_2H_2. Table 3 gives the calculated bond dissociation energies (BDE) for the reaction Pb_2X_2 (**E**) → 2PbX($X^2\Pi$). Subtracting the excitation energies for 2 PbX moieties from the BDE gives highly negative values which means that Pb_2X_2 (**E**) is much higher in energy than the PbX fragments in the electronic ground state. With other words, energetically favourable dimers XPbPbX can only be formed using PbX in the $X^2\Pi$ ground state.

Figures 3a–c show two PbX species in the $X^2\Pi$ ground state, which are connected to each other in different orientations where the unpaired electrons yield an electron-sharing σ bond. The orientation 3a leads to structure **F2** which has only a Pb–Pb σ bond. A much more favourable orientation of the two fragments is shown in 3b which arises from 3a after the rotation about the Pb–Pb axis by 90°. The Pb–X bonds can interact with the empty $p(\pi)$ AO of the other PbX fragment which leads to the butterfly structure **A**. Tilting of the Pb–X bonds yields two donor–acceptor bonds which enhance the Pb–Pb bonding interactions. Structure **A** possesses three Pb–Pb electron-pair bonding contributions, i.e. one electron-sharing σ bond and two degenerate donor–acceptor bonds. Note that the alternative donor–acceptor bond from the electron lone-

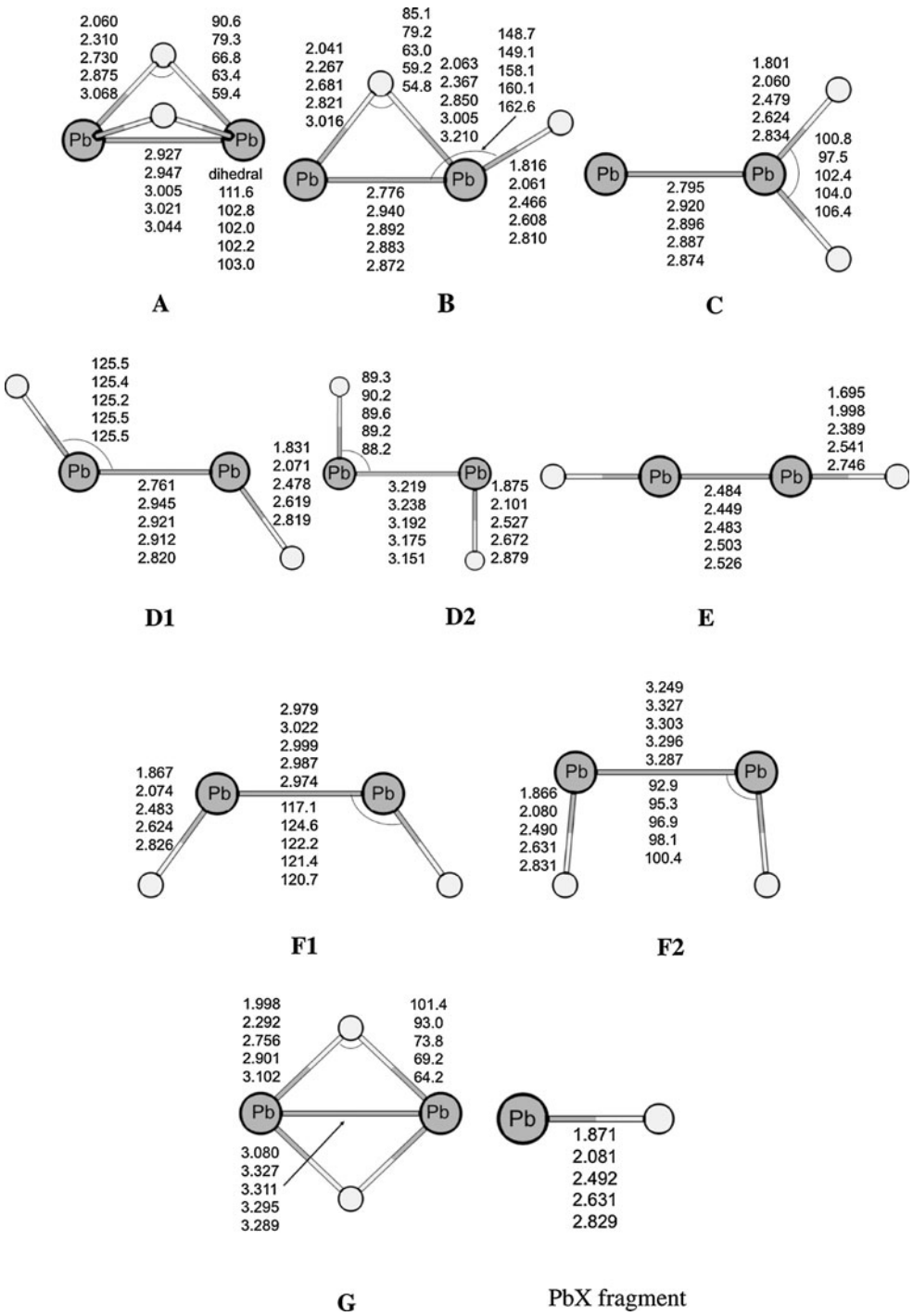

Fig. 1 Optimized geometries of Pb_2X_2 isomers **a**–**g** and the PbX fragment in the $X^2\Pi$ ground state calculated at BP86/QZ4P. Values from *top* to *bottom*: X = H, F, Cl, Br, I. Bond lengths are given in Å, and angles are given in degrees

pairs at Pb in Fig. 3b is less favourable because the E–X bonds are better electron donors than electron lone-pairs for atoms E = Si–Pb. Figure 3c shows a similar bonding situation as in Fig. 3a yielding the trans form **D2** which has also only an electron-sharing σ bond.

Figures 3d–g show two PbX species in different orientations where the unpaired electrons yield an electron-sharing Pb–Pb π bond. The orientation in Fig. 3d leads to structure **B** where the π bond becomes completed with a lone-pair donor–acceptor σ bond and with a PbX donor–acceptor bond where one Pb–X bond is tilted towards the empty $p(\pi)$ AO of the other PbX fragment. Thus, structure **B** has like **A** three electron-pair Pb–Pb bonding components: one π bond, one lone-pair donor–acceptor σ bond and one PbX donor–acceptor bond. The orientation in Fig. 3e leads in a similar fashion to structure **G** which possesses an electron-sharing π bond and two PbX donor acceptor bonds. The donation of the lone-pair orbitals

Table 1 Relative energies of the **A**–**G** isomers of Pb_2X_2 calculated with BP86/QZ4P and ab initio methods with aug-cc-pVQZ basis sets

	H	F	Cl	Br	I	H	F	Cl	Br	I
	A					**B**				
BP86	0 (0)	0 (0)	0 (0)	0 (0)	0 (0)	17.0 (1)	31.8 (1)	34.0 (1)	33.9 (1)	33.4 (1)
MP2	0	0	0	0	0	18.2	31.4	35.8	37.2	36.9
SCS-MP2	0	0	0	0	0	18.1	31.3	35.3	36.8	36.4
MP4	0	0	0	0	0	17.3	29.9	33.6	35.5	35.4
CCSD(T)	0	0	0	0	0	16.8	29.5	33.1	35.0	35.0
	C					**D1**				
BP86	27.1 (2)	43.7 (2)	45.3 (2)	45.6 (2)	46.0 (2)	31.0 (2)	38.2 (2)	38.4 (2)	38.4 (2)	38.5 (2)
MP2	27.5	40.3	45.8	48.6	50.1	33.4	38.9	43.1	44.8	45.7
SCS-MP2	26.0	40.0	44.0	46.9	48.1	32.2	38.5	41.9	43.5	44.2
MP4	25.9	39.6	43.3	46.7	48.1	31.2	36.5	40.5	42.6	43.3
CCSD(T)	24.5	39.1	42.2	45.5	46.7	30.1	36.8	39.9	41.8	42.5
	D2					**E**				
BP86	26.5 (1)	18.8 (1)	19.2 (1)	20.0 (1)	20.7 (1)	92.5 (2)	198.1 (2)	170.1 (2)	160.6 (2)	145.5 (2)
MP2	26.4	18.1	20.2	22.6	24.6	85.2	190.5	179.8	163.2	143.3
SCS-MP2	22.8	17.2	17.4	19.9	21.6	87.1	191.8	182.9	165.0	143.8
MP4	24.7	18.5	18.3	21.2	23.0	86.1	184.2	180.3	162.6	141.3
CCSD(T)	23.3	18.3	17.3	20.1	21.6	86.6	181.1	160.2	152.1	139.5
	F1					**F2**				
BP86	47.7 (2)	41.4 (2)	42.0 (2)	42.2 (2)	42.5 (2)	27.9 (1)	23.2 (1)	24.2 (1)	24.9 (1)	26.0 (1)
MP2	51.2	42.6	51.5	49.3	51.0	28.1	23.5	26.5	28.5	30.4
SCS-MP2	48.8	41.8	49.4	47.9	49.3	24.4	22.3	23.7	25.9	27.6
MP4	47.6	39.4	46.1	46.5	47.9	26.2	23.1	24.3	26.8	28.5
CCSD(T)	43.9	38.7	42.0	44.9	46.3	24.8	23.1	23.4	25.8	27.2
	G									
BP86	4.4 (1)	22.4 (1)	32.7 (1)	34.2 (1)	35.4 (1)					
MP2	3.8	22.8	33.4	36.4	45.4					
SCS-MP2	4.4	22.1	33.0	36.2	45.0					
MP4	3.9	16.5	28.6	32.6	44.2					
CCSD(T)	4.0	12.8	26.5	31.1	43.7					

The relative energies with respect to **A** are given in kcal/mol. The values in parentheses are the number of imaginary frequencies

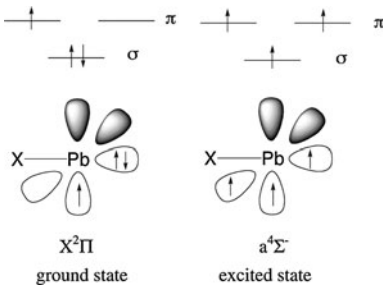

Fig. 2 Schematic representation of the $X^2\Pi$ ground state and the $a^4\Sigma^-$ excited state of PbX

rather than PbX bonds (Fig. 3f) leads to the trans-bent structure **D1**. The latter structure should be less stable than **G** because the donation from E–X bonds is more favourable than the donation lone-pair orbitals for Si–Pb. Table 1 shows that structure **G** is always lower in energy than **D1**.

Table 2 Calculated excitation energies from the $X^2\Pi$ ground state to the $a^4\Sigma^-$ excited state at BP86/QZ4P, MRCI-SD/aug-cc-pvQZ//BP86/QZ4P and MRCI-SD(Q)/aug-cc-pvQZ//BP86/QZ4P levels, where (Q) indicates the inclusion of the Davidson correction

	BP86/QZ4P	MRCI-SD/aug-cc-pVQZ	MRCI-SD(Q)/aug-cc-pVQZ
PbH	52.0	50.2	50.7
PbF	109.4	110.2	113.5
PbCl	90.3	92.5	94.0
PbBr	77.6	82.0	83.7
PbI	65.8	74.6	75.0

The energies are given in kcal/mol

The latter structure may become favourable for systems REER with large substituents R which are subject to strong steric repulsion [27]. Note that the trans-bent form **D1**,

Table 3 Calculated dissociation energies D_e of the linear X–Pb≡Pb–X into 2 PbX molecules and the excitation energies from the $X^2\Pi$ ground state to the $a^4\Sigma^-$ excited state of the PbX molecules at BP86/QZ4P

	D_e	ΔE_{exc}	$D_e - 2\Delta E_{exc}$
H	69.0	52.0	−35.0
F	69.0	109.4	−149.8
Cl	59.5	90.3	−121.1
Br	45.4	77.6	−109.9
I	38.4	65.8	−93.1

The energies are given in kcal/mol

which has three bonding components (one electron-sharing π bond and two lone-pair donor–acceptor bonds), is higher in energy than the trans-bent form **D2** which has one electron-sharing σ bond. Finally, Fig. 3g leads to structure **F1** which is the syn homologue of the trans-bent form **D1** possessing one electron-sharing π bond and two lone-pair donor–acceptor bonds.

Table 4 gives the results of the EDA calculations of Pb_2X_2 isomers **A**–**G**. The interacting fragments are two PbX diatomics in the $X^2\Pi$ ground state except for the linear structure **E** where PbX in the $a^4\Sigma^-$ excited state has been chosen. Although most structures are no minima on the PES, the calculated data give valuable information about the strength of the different components of the Pb–Pb interactions. In particular, the strength of the various types of orbital interactions can be estimated in Pb_2X_2 for different atoms X.

The comparison of the results for the global energy minima **A** shows that the BDE for the Pb–Pb bond changes only slightly for different X. The largest value is calculated for Pb_2H_2 ($D_e = 57.5$ kcal/mol). The BDEs of the halogen systems Pb_2X_2 increase in the order F ($D_e = 48.3$ kcal/mol) < Cl ($D_e = 49.8$ kcal/mol) < Br ($D_e = 50.8$ kcal/mol) < I ($D_e = 52.2$ kcal/mol). Note that the instantaneous interaction energy ΔE_{int} has rather uniform values for all systems which vary between $\Delta E_{int} = -64.3$ kcal/mol for Pb_2H_2 and $\Delta E_{int} = -60.8$ kcal/mol for Pb_2Br_2. The percentage contributions of the energy terms to ΔE_{int} also change very little which means that the nature of the bonding in Pb_2X_2 (**A**) is rather independent from X. The electrostatic term ΔE_{elstat} and the orbital (covalent) term ΔE_{orb} have similar strengths.

Structure **B** has C_s symmetry and therefore, the contribution of the "a" orbitals to ΔE_{orb} gives the strength of the $p(\pi)$ electron-sharing bond (Fig. 3d) [see footnote 1] [1].

[1] Structure A has also Cs symmetry. However, the EDA requires that the fragments have the same symmetry with regard to the whole molecule. The fragments PbX in structure A have C1 symmetry with regard to the mirror plane of the Cs symmetric Pb_2X_2 (A).

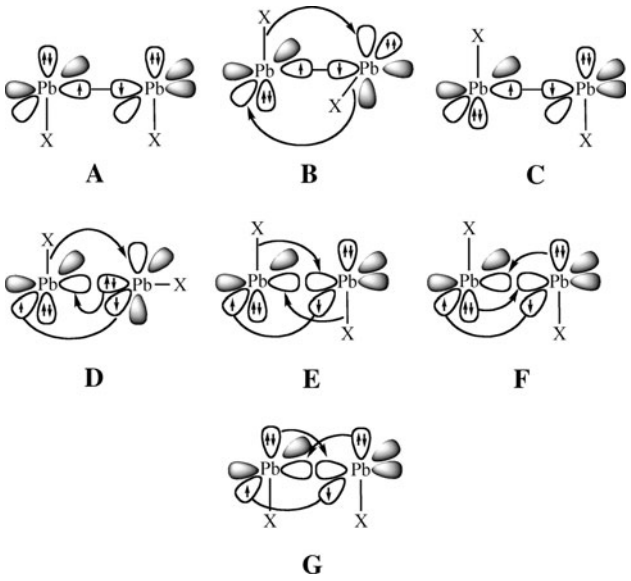

Fig. 3 Qualitative model for the orbital interactions between two PbX molecules in different orientations where the unpaired electrons of **a**–**c** yield an electron-sharing σ bond and where those of **d**–**g** yield an electron-sharing π bond

Table 4 shows that the latter term contributes between 27.5% (Pb_2H_2) and 38.1% (Pb_2F_2) to the total orbital interactions. Structure **D1** possesses also an $p(\pi)$ electron-sharing bond (Fig. 3f), which has about the same strength as the $p(\pi)$ bond in **B**. The percentage contribution of the $p(\pi)$ bond in **D1** is higher (between 39.1 and 58.1%) than in **B** (between 27.5 and 38.1%) because the other two orbital contributions in the former structure (two lone-pair donor–acceptor bonds) are weaker than the orbital interactions in the latter (one lone-pair σ bond and one PbX donor–acceptor bond).

The trans-bent structure **D2** has only one bonding contribution from orbital interactions (Fig. 3c) and yet, the Pb–Pb bond is stronger than in the trans-bent structure **D1** which has three orbital components. One reason for the finding is that the latter structure has a much stronger electrostatic term ΔE_{elstat} than the former. This compensates in the parent system Pb_2H_2 for the overall weaker orbital interactions in **D2** than in **D1**. The energy difference between the trans-bent forms **D1** and **D2** of the halogen systems Pb_2X_2 are much larger than for Pb_2H_2. This is because the strength of the electron-sharing σ bond in the **D2** structure of the former systems is between 44.8 kcal/mol (Pb_2F_2) and 51.9 kcal/mol (Pb_2I_2) while the three components in **D1** (one $p(\pi)$ electron-sharing bond and two lone-pair donor–acceptor bonds) are altogether weaker than in **D2**. The conclusion is that the lone-pair donor–acceptor interactions in the halogen systems of Pb_2X_2 is very weak.

The strength and the nature of the bonding interactions in the linear form **E** varies very little for all systems Pb_2X_2

Table 4 Energy decomposition analysis of the investigated Pb_2X_2 at BP86/QZ4P level of the Pb–Pb bond using two ($X^2\Pi$) doublet fragments for **A–G**

Term	A	B	D1	D2	E	F1	F2	G
Pb_2H_2								
ΔE_{int}	−64.3	−44.2	−27.8	−32.0	−81.1	−10.8	−30.5	−56.9
ΔE_{Pauli}	229.4	138.1	77.4	74.8	117.4	36.0	71.1	149.2
ΔE_{elstat}	−134.9	−94.1	−45.7	−61.8	−73.4	−12.4	−58.1	−109.3
	45.9%	51.6%	43.5%	58.0%	37.0%	26.5%	57.2%	53.0%
ΔE_{orb}	−158.8	−88.1	−59.5	−45.0	−125.1	−34.4	−43.5	−96.9
	54.1%	48.4%	56.5%	42.1%	63.0%	73.5%	42.8%	47.0%
$\Delta E_{orb}(a')$		−63.9	−36.2	−44.8	−73.0	−16.7	−43.4	−78.7
		72.5%	61.0	99.7%	55.0%	48.6%	99.7%	81.3%
$\Delta E_{orb}(a'')$		−24.3	−23.2	−0.1	−59.7	−17.7	−0.1	−18.2
		27.5%	39.1%	0.3%	45.0%	51.4%	0.3%	18.8%
ΔE_{prep}	6.8	3.7	1.3	1.0	116.2	1.0	1.0	3.9
$\Delta E(=-D_e)$	−57.5	−40.4	−26.5	−31.0	−35.0	−9.8	−29.5	−53.1
Pb_2F_2								
ΔE_{int}	−62.7	−22.3	−11.1	−30.6	−80.2	−7.9	−26.1	−38.7
ΔE_{Pauli}	194.6	82.5	32.4	77.6	79.2	25.6	66.3	112.6
ΔE_{elstat}	−125.3	−48.3	−7.8	−63.0	−26.7	−3.2	−51.3	−93.1
	48.7%	46.1%	17.8%	58.3%	16.8%	9.6%	55.5%	61.5%
ΔE_{orb}	−132.1	−56.5	−35.7	45.1	−132.6	−30.3	−41.1	−58.3
	51.3%	53.9%	82.2%	41.7%	83.2%	90.5%	44.5%	38.5%
$\Delta E_{orb}(a')$		−35.0	−15.0	−44.8	−73.0	−11.6	−40.8	−55.9
		61.9%	41.9%	99.2%	55.1%	38.2%	99.3%	95.9%
$\Delta E_{orb}(a'')$		−21.5	−20.8	−0.4	−59.7	−18.7	−0.3	−2.4
		38.1%	58.1%	0.8%	45.0%	61.8%	0.7%	4.1%
ΔE_{prep}	14.4	5.8	1.0	1.1	230.0	1.0	0.9	12.7
$\Delta E(=-D_e)$	−48.3	−16.5	−10.1	−29.5	149.8	−6.9	−25.2	−26.0
Pb_2Cl_2								
ΔE_{int}	−60.9	−20.19	−11.8	−31.9	−90.9	−8.8	−26.6	−29.6
ΔE_{Pauli}	204.4	83.30	38.8	84.0	83.7	29.1	67.6	107.3
ΔE_{elstat}	−126.0	−42.93	−14.6	−67.2	−34.4	−4.9	−51.7	−74.0
	47.5%	41.48%	28.8%	58.0%	19.7%	12.8%	54.8%	54.0%
ΔE_{orb}	−139.2	−60.57	−36.0	−48.7	−140.2	−33.1	−42.6	−63.0
	52.5%	58.52%	71.2%	42.0%	80.3%	87.2%	45.2%	46.0%
$\Delta E_{orb}(a')$		−38.56	−16.0	−47.9	−74.5	−14.0	−42.1	−57.2
		63.67%	44.4%	98.5%	53.2%	42.4%	98.8%	90.8%
$\Delta E_{orb}(a'')$		−22.00	−20.0	−0.7	−65.7	−19.0	−0.5	−5.8
		36.32%	55.6%	1.5%	46.9%	57.7%	1.2%	9.3%
ΔE_{prep}	11.1	4.36	0.4	1.3	212.0	1.1	1.0	12.5
$\Delta E(=-D_e)$	−49.8	−15.8	−11.4	−30.6	121.1	−7.8	−25.6	−17.1
Pb_2Br_2								
ΔE_{int}	−60.8	−20.9	−13.5	−32.3	−83.6	−9.7	−27.0	−28.3
ΔE_{Pauli}	209.5	86.3	40.1	88.2	83.0	31.1	68.9	108.2
ΔE_{elstat}	−130.8	−44.6	−13.0	−70.1	−34.6	−6.5	−52.7	−71.7
	48.4%	41.6%	24.3%	58.2%	20.8%	15.9%	55.0%	52.6%
ΔE_{orb}	−139.4	−62.7	−40.6	−50.4	−131.9	−34.3	−43.2	−64.8
	51.6%	58.4%	75.4%	41.8%	79.2%	84.1%	45.0%	47.5%
$\Delta E_{orb}(a')$		−40.7	−19.3	−49.4	−68.9	−15.2	−42.5	−57.9
		64.9%	47.6%	98.1%	52.2%	44.2%	98.5%	89.4%

Table 4 continued

Term	A	B	D1	D2	E	F1	F2	G
$\Delta E_{orb}(a'')$		−22.0	−21.3	−1.0	−63.1	−19.1	−0.6	−6.9
		35.1%	52.4%	1.9%	47.8%	55.8%	1.5%	10.6%
ΔE_{prep}	10.0	4.0	1.1	1.4	193.4	1.1	1.1	11.7
$\Delta E(=-D_e)$	−50.8	−16.9	−12.4	−31.0	109.9	−8.6	−25.9	−16.5
Pb_2I_2								
ΔE_{int}	−60.9	−22.5	−14.9	−33.1	−75.6	−10.9	−27.3	−27.3
ΔE_{Pauli}	215.1	91.7	44.2	94.2	84.2	34.1	70.1	110.1
ΔE_{elstat}	−134.9	−47.9	−16.2	−74.0	−36.7	−8.7	−53.5	−70.1
	48.9%	42.0%	27.4%	58.1%	22.9%	19.4%	55.0%	51.0%
ΔE_{orb}	−141.1	−66.2	−43.0	−53.3	−123.1	−36.3	−43.9	−67.3
	51.12%	58.0%	72.6%	41.9%	77.0%	80.6%	45.1%	49.0%
$\Delta E_{orb}(a')$		−44.1	−21.6	−51.9	−63.0	−17.1	−43.1	−58.9
		66.6%	50.3%	97.3%	51.2%	47.1%	98.1%	87.6%
$\Delta E_{orb}(a'')$		−22.1	−21.4	−1.5	−60.0	−19.2	−0.8	−8.3
		33.4%	49.7%	2.7%	48.7%	52.9%	1.9%	12.4%
ΔE_{prep}	8.6	3.6	1.2	1.6	168.7	1.2	1.1	10.5
$\Delta E(=-D_e)$	−52.2	−18.8	−13.8	−31.5	93.1	−9.8	−26.2	−16.8

Two ($a^4\Sigma^-$) quartet fragments are used for **E**. The symmetry in the analysis is C_s except for the **A** isomer. All energies are given in kcal/mol

(Table 4). As mentioned above, the halogen systems are even more unstable than the parent hydrogen system because the former compounds have higher $a^4\Sigma^- \leftarrow X^2\Pi$ excitation energies. This shows up in the EDA calculations through the much higher ΔE_{prep} values and the strongly negative BDEs of Pb_2X_2 (X = F–I). The syn-bent structure **F1** and **F2** exhibit similar EDA values as the related trans-bent forms **D1** and **D2**. Thus, the Pb–Pb bond in all structures Pb_2X_2 (**F1**) is weaker than in **F2**.

5 Summary

The results of this work can be summarized as follows. The energy minimum structures of the halogen substituted Pb_2X_2 molecules possess a doubly bridged butterfly geometry **A** like the parent system Pb_2H_2. The unusual geometry can be explained with the interactions between PbX fragments in the $X^2\Pi$ ground state which leads to one Pb–Pb electron-sharing σ bond and two donor–acceptor bonds between the Pb–X bonds as donor and vacant $p(\pi)$ AOs of Pb. The energy difference between the equilibrium form A and the linear structure XPb≡PbX (E) which is a second-order saddle point is much higher when X is a halogen atom than for X = H. This is because the $a^4\Sigma^- \leftarrow X^2\Pi$ excitation energies of PbX (X = F–I) are higher than for PbH. The structural isomers **B**, **D1**, **D2**, **E**, **F1**, **F2** and **G** of Pb_2X_2 are no minima on the potential energy surface.

Acknowledgments This work was supported by the Deutsche Forschungsgemeinschaft.

References

1. Weidenbruch M (2003) Angew Chem Int Ed 42:2222
2. Weidenbruch M (2002) J Organomet Chem 646:39
3. Power PP (1999) Chem Rev 99:3463
4. Lawrence SC, Wasserman ZR, Moskowitz JW (1982) Int J Quantum Chem 21:565
5. Lischka H, Köhler H (1983) J Am Chem Soc 105:6646
6. Binkley JS (1984) J Am Chem Soc 106:603
7. Köhler HJ, Lischka H (1984) Chem Phys Lett 112:33
8. Clabo DA, Schaefer HF (1986) J Chem Phys 84:1664
9. Luke BT, Pople JA, Krogh-Jespersen MB, Apeloig Y, Karni M, Chandrasekhar J, Schleyer PvR (1986) J Am Chem Soc 108:270
10. Koseki S, Gordon MS (1988) J Phys Chem 92:364
11. Koseki S, Gordon MS (1989) J Phys Chem 93:118
12. Sax AF, Kalcher J (1990) J Mol Struct Theochem 208:123
13. Colegrove BT, Schaefer HF (1990) J Phys Chem 94:5593
14. Grev RS (1991) Adv Organomet Chem 33:125
15. Grev RS, Schaefer HF (1992) J Chem Phys 97:7990
16. Hühn MM, Amos RD, Kobayashi R, Handy NC (1993) J Chem Phys 98:7107
17. Yamaguchi Y, Deleeuw BJ, Richards CA, Schaefer HF, Frenking G (1994) J Am Chem Soc 116:11922
18. Jursic BS (1999) J Mol Struct Theochem 491:1
19. Jursic BS (2000) J Mol Struct Theochem 497:65
20. Krüger T, Sax AF (2001) J Comput Chem 22:151
21. Nagase S, Kobayashi K, Takagi N (2000) J Organomet Chem 611:264
22. Takahashi M, Kawazoe Y (2000) Organometallics 611:264
23. Damrauer R, Noble AL (2008) Organometallics 27:1707
24. Dolgonos G (2008) Chem Phys Lett 454:190
25. Dolgonos G (2008) Chem Phys Lett 457:453

26. Han YK, Bae C, Lee YS, Lee SY (1998) J Comput Chem 19:1526
27. Chen Y, Hartmann M, Diedenhofen M, Frenking G (2001) Angew Chem Int Ed 40:2052
28. Bridgtman AJ, Ireland LR (2001) Polyhedron 20:2841
29. Bogey M, Bolvin H, Demuyneck C, Destombes JL (1991) Phys Rev Lett 66:413
30. Wang X, Andrews L, Kushto G (2002) J Phys Chem A 106:5809
31. Wang X, Andrews L, Chertihin GV, Souer PF (2002) J Phys Chem A 106:6302
32. Wang X, Andrews L (2003) J Am Chem Soc 125:6581
33. Pu L, Twamley B, Power PP (2000) J Am Chem Soc 122:3524
34. Jung Y, Brynda M, Power PP, Head-Gordon M (2006) J Am Chem Soc 128:7185
35. Lein M, Krapp A, Frenking G (2005) J Am Chem Soc 127:6290
36. Takahashi M, Sakamoto K (2004) J Phys Chem A 108:5710
37. Takahashi M, Kawazoe Y (2008) Organometallics 27:4829
38. Li G, Li Q, Xu W, Xie Y, Schaefer HF (2001) Mol Phys 99:1053
39. Li Q, Li G, Xu W, Xie Y, Schaefer HF (2002) Chem Phys Chem 3:179
40. Becke AD (1988) Phys Rev A 38:3098
41. Perdew JP (1986) Phys Rev B 33:8822
42. Perdew JP (1986) Phys Rev B 34:7406
43. Snijders JG, Baerends EJ, Vernooijs P (1982) At Nucl Data Tables 26:483
44. Snijders JG, Baerends EJ (1978) Mol Phys 36:1789
45. ADF 2007.01, SCM, *Theoretical chemistry*. Vrije Universiteit, Amsterdam. http://www.scm.com
46. Møller C, Plesset MS (1934) Phys Rev 46:618
47. Grimme S (2003) J Chem Phys 118:9095
48. Krishnan R, Pople JA (1978) Int J Quantum Chem 14:91
49. Čížek J (1960) J Chem Phys 45:4256
50. Čížek J (1969) Adv Chem Phys 14:35
51. Bartlett J (1989) Ann Rev Phys Chem 32:359
52. Dunning TH (1989) J Chem Phys 90:1007
53. Wilson AK, Woon DE, Peterson KA, Dunning TH Jr (1999) J Chem Phys 110:7667
54. Peterson KA (2003) J Chem Phys 119:11099
55. Metz B, Stoll H, Dolg M (2000) J Chem Phys 113:2563
56. Lie GC, Hinze J (1973) J Chem Phys 59:1872
57. Buenker RJ, Peyerimhoff SD (1974) Theor Chim Acta 35:33
58. Schmidt MW, Gordon MS (1998) Annu Rev Phys Chem 49:233
59. Langhoff SR, Davidson ER (1974) Int J Quantum Chem 8:61
60. Werner HJ, Knowles PJ, Lindh R, Manby FR, Schütz M, Celani P, Korona T, Rauhut G, Amos RD, Bernhardsson A, Berning A, Cooper DL, Deegan MJO, Dobbyn AJ, Eckert F, Hampel C, Hetzer G, Lloyd AW, McNicholas SJ, Meyer W, Mura ME, Nicklass A, Palmieri P, Pitzer R, Schumann U, Stoll H, Stone AJ, Tarroni R, Thorsteinsson T, MOLPRO, version 2006.1, a package of ab initio programs. See. http://www.molpro.net
61. Morokuma K (1971) J Chem Phys 55:1236
62. Ziegler T, Rauk A (1977) Theor Chim Acta 46:1
63. Zhurko GA, Chemcraft. See. http://www.chemcraftprog.com
64. Huber KP, Herzberg G (1979) Molecular spectra and molecular structure IV. Constants of diatomic molecules. Van Nostrand-Reinhold, New York
65. Watson WW (1938) Phys Rev 54:1068
66. Watson WW, Simon R (1940) Phys Rev 57:708
67. Kleman B (1953) Ph.D. Thesis, Stockholm
68. Balasubramanian K, Pitzer KS (1984) J Phys Chem 88:1146